Published: 7th October 2026

ANACHEM JOURNAL
ISSN: 2006-5221 (Online)

SYNERGISTIC EFFECTS OF ECO-FRIENDLY MORINGA LEAF EXTRACT AND SYNTHETIC INHIBITOR BLENDS ON MILD STEEL CORROSION IN PETROLEUM-PRODUCED WATER

[1]Odisu, T., [*1]Akakabota, A.O., [1] Ovuoraye, P. E., and [1]Ofotobor, P.

[1]Department of Chemical Engineering, Federal University of Petroleum Resources, P.M.B. 1221, Effurun, Nigeria.
***Corresponding author's e-mail:** akakabota.ambrose@fupre.edu.ng

https://doi.org/10.5281/zenodo.23129951

ABSTRACT

The high salinity and ionic content of petroleum produced water make it a challenging medium, hence necessitating inhibitors that can withstand aggressive conditions. This study evaluated a blend of Moringa leaf extract and a water-based corrosion inhibitor for inhibiting corrosion of mild steel in petroleum produced water at temperatures from 313K to 353K, immersion times of 2 to 10 days, and inhibitor concentrations from 0ppm to 100ppm. Polished mild steel coupons were immersed in 50 mL of produced water with varying concentrations (0/100ppm, 25/75ppm, 50/50ppm, 75/25ppm, and 100/0ppm) of inhibitor blend at 30°C. After immersion, the coupons were cleaned and weighed to assess corrosion by weight loss. The samples were characterized using FTIR and SEM-EDX. Results showed that inhibition efficiency (% IE) decreased as temperature increased. At lower temperatures (40°C and 50 °C), higher Moringa leaf extract concentrations yielded up to 83.33% efficiency, while at higher temperatures (70°C and 80°C), efficiency dropped, with pure Moringa extract achieving only 70% at 70°C. The blends formed protective films on the steel surface, with the 25/75 blend showing the highest activation energy (38.392 kJ/mol), indicating superior thermal stability. Thermodynamic parameters indicated an endothermic corrosion process and successful Langmuir adsorption fitting, highlighting Moringa leaf extract's potential as a bio-based corrosion inhibitor in industrial applications.

Keywords: Corrosion inhibitor, Moringa extract, Adsorption, Petroleum produced water, Scanning electron microscopy (SEM) and energy-dispersive X-ray (EDX)

1.0 Introduction

Corrosion of mild steel in industrial environments, particularly in oil and gas production, poses significant economic and safety challenges (Popoola et al., 2013). Petroleum produced water, a byproduct of oil extraction, contains high concentrations of chloride ions, sulfates, and other corrosive species that accelerate metal degradation (Jain et al., 2017). Mild steel, widely used in pipelines and structural components due to its cost-effectiveness and mechanical properties, is highly susceptible to corrosion in such aggressive environments (Udounwa & Wilson, 2025).

Petroleum produced water, a complex aqueous stream generated during oil and gas extraction, contains high concentrations of chloride ions, sulphates, total dissolved solids, CO_2, H_2S, and hydrocarbons that can accelerate metallic degradation (Bhutani et al., 2024). This type of environment can lead to uniform corrosion, pitting, and microbiologically influenced corrosion (MIC) through processes such as anodic dissolution ($Fe \rightarrow Fe^{2+} + 2e^-$) and cathodic hydrogen evolution or oxygen reduction (Emmanuel, 2024). Chloride ions and sulfates can exacerbate the issue by disrupting the protective oxide layers on steel surfaces (Jee & Pradhan, 2022). In fact, the oil sector faces annual corrosion-related economic losses exceeding $60 billion, highlighting the urgent need for effective prevention strategies (Prasad et al., 2020).

Mild steel, a low-carbon alloy is commonly used in the oil and gas industry for applications such as pipelines, storage tanks, and drilling equipment, is particularly susceptible to corrosion, especially in harsh environments like produced water (Al-Janabi, 2020). The need for effective, eco-friendly corrosion inhibitors has driven research towards natural extracts, which offer sustainable alternatives to synthetic inhibitors (Njoku et al., 2024). Because synthetic chemicals used as corrosion inhibitors are not green and are highly expensive, coupled with significant environmental concerns (Aghogho et al., 2025), the need for development of effective, eco-friendly corrosion inhibitors has driven research towards natural extracts, which offer sustainable alternatives to synthetic inhibitors (Njoku et al., 2024).

Moringa oleifera is a phytochemically rich plant that has attracted considerable interest as a potential green corrosion inhibitor. Its leaves contain various bioactive constituents, including flavonoids, alkaloids, and phenolic acids, which contain functional groups that may interact with and adsorb onto metal surfaces, thereby forming protective layers that mitigate corrosion (Mustapha et al., 2024). Previous studies have demonstrated the efficacy of plant-based extracts in inhibiting corrosion in acidic and saline environments (Dehghani et al., 2024; Elijah et al., 2025). For instance, Didouh *et al.* (2023) reported that Moringa leaf extract effectively reduced corrosion rates in mild steel exposed to acidic media by forming a stable adsorptive film. To combat corrosion in produced water, chemical additives cling to the metal surface, creating a protective barrier (Makhlouf et al., 2018). While traditional synthetic inhibitors, such as imidazolines and quaternary ammonium salts, can be highly effective, achieving efficiencies of up to 95%, they often come with downsides, including toxicity, environmental persistence, and high costs (Fedorowicz & Saczewski, 2024). This has driven growing interest in more eco-friendly alternatives (Ahmed et al., 2024; Hossain et al., 2021).

Additionally, natural inhibitors from plant extracts, which are rich in heteroatoms (such as nitrogen, oxygen, and sulfur) and π-electrons, offer eco-friendly, low-toxicity alternatives that perform comparably to synthetic agents, especially when blended for enhanced effects (Ahmed et al., 2024). These compounds can attach through physisorption (an electrostatic process) or chemisorption (involving charge transfer), following Langmuir or Temkin isotherms, and lower corrosion rates by blocking active sites (Akalezi et al., 2020).

Research on Moringa leaf extract (MLE) for mild steel corrosion mainly targets acidic environments (like 1 M HCl or H_2SO_4), where it shows mixed-type inhibition

(affecting both anodic and cathodic reactions) with efficiencies reaching up to 93% at 1.5 g/L (Akalezi et al., 2020). However, high salinity and CO_2 in produced water could hinder MLE's effectiveness, so blending it with other substances may be necessary for better stability (Azeem et al., 2023). Combining natural extracts like MLE with synthetic water-based inhibitors creates a powerful synergy (Zhang et al., 2023): the natural phenolics enhance adsorption density, while the synthetics provide thermal stability and improved dispersibility.

Despite the increasing use of plant extracts as corrosion inhibitors, research on blends of moringa extract and synthetic inhibitors in environments such as petroleum-produced water remains limited. Corrosion follows kinetic and thermodynamic principles that govern the rate and spontaneity of metal degradation (Quadri et al., 2022). Activation energy (Ea) reflects the energy barrier for corrosion reactions. In contrast, thermodynamic parameters such as enthalpy (ΔH^o), entropy (ΔS^o), and Gibbs free energy (ΔG^o) provide insights into the reaction's nature and inhibitor performance (Toghan et al.,2023). Adsorption isotherms, such as the Langmuir, Freundlich, and Temkin models, model the interaction between inhibitors and metal surfaces and provide a deeper understanding of inhibition mechanisms (Ituen et al., 2017). The Langmuir isotherm, in particular, assumes monolayer adsorption, which is often observed in plant-based inhibitors due to their polar functional groups (Nyangiwe, 2025).

This research investigated the synergistic effects of a blend of Moringa leaf extract (MLE) and a water-based inhibitor (a blend of polyamine and surfactant) on the corrosion inhibition of mild steel in petroleum-produced water. The study also used scanning electron microscopy (SEM), Fourier transform infrared (FTIR) spectroscopy, and energy-dispersive X-ray spectroscopy (EDX) to assess protective film formation and elemental changes on the steel surface. Additionally, the study examined the impact of corrosion-inhibition variables, as well as the mechanistic and thermodynamic aspects of blending MLE with a water-based inhibitor in petroleum-produced water. By examining kinetic and thermodynamic parameters, as well as adsorption behavior, this research aims to elucidate the inhibition mechanisms of MLE and its blends and contribute to the development of sustainable corrosion mitigation strategies for oilfield applications.

2.0 Materials and Methods

2.1 Collection and Preparation of Samples

The following materials/ apparatus were used for the experiment. The Moringa (*Moringa Oleifera)* leaves were sourced from Ugbomro town in Effurun, Delta State, Nigeria. The mild steel was procured in Effurun and processed using an industrial particle-size reduction machine in the Mechanical workshop in Ugbomro. The produced water was obtained from a petroleum exploration field X located in Delta State, Nigeria. The analytical grade reagents used in this work included ethanol (98% purity), a blended formulation of polyamine and surfactant, acetone (95% purity), and distilled water. The moringa leaves were thoroughly cleaned under running water. After 14 days of outdoor drying, the cleaned sample was ground into a fine powder using an industrial blender until the particle size was 0.143 u̧m.

2.2 Extraction procedure

Following the procedure implemented by Okewale and Adesina (2020), the moringa leaves were washed to remove dirt and air-dried for 14 days. A cellulose thimble

containing 50g of dried and powdered Moringa leaves was put inside the Soxhlet extractor. A round-bottom flask was filled with 250 millilitres of ethanol and connected to the condenser and Soxhlet extractor. The ethanol was allowed to evaporate, condense, and drip over the leaf powder by gently heating the system using a heating mantle. After approximately six hours of solvent-extraction cycles, the ethanol in the syphon tube appeared clear, indicating that all the bioactive chemicals had been extracted. After extraction, the apparatus was allowed to cool to room temperature. The ethanol extract solution was collected and concentrated by evaporating the ethanol using a rotary evaporator for further analysis; the concentrated extract was stored in a sealed container at refrigeration temperature. Mild steel coupons were immersed for 2, 4, 6, 8, and 10 days to study the impact of immersion time on corrosion rates. The corrosion rate was measured at 313K, 323K, 333K, 343K, and 353K for a constant 10-hour period to assess the effect of temperature on corrosion. Various concentrations (0/100ppm, 25/75ppm, 50/50ppm, 75/25ppm, 100/0ppm) of the Moringa leaf extract and water-based inhibitor blend were used to evaluate their effectiveness in corrosion inhibition.

2.3 Characterization of the Moringa Leaf Extract

2.3.1 Phytochemical analysis

Physicochemical properties and phytochemical constituents of the moringa leaf extract were screened to identify the active constituents present.

Scanning electron microscopy (SEM) and energy-dispersive X-ray (EDX) analyses were also carried out on the MLE and mild steel specimen. The mild steel specimen was cleaned with distilled water and acetone, air-dried, and then submerged in the test media (produced water with and without an inhibitor) for seven days to monitor changes in surface morphology. The specimen's surface morphology was then examined using a scanning electron microscope (SEM), which generates images by scanning a sample with a focused electron beam (Afoegba et al., 2020).

Fourier transform infrared (FTIR) spectroscopy was employed to identify the functional groups present in the Moringa leaf extract and the water-based inhibitor. This technique provides crucial insights into the extract's chemical composition and potential interactions with mild steel in corrosive environments. Moringa leaves (*Moringa Oleifera*) (0.143 µm particle size) were analyzed using FTIR spectroscopy (Buck Scientific model 530) in the range 650-4000 cm^{-1} (wavenumber). The background material used in the analysis is potassium bromate (KBr).

2.3.2 Corrosion study

The corrosion study followed the method reported by Nwigbo et al. (2012) and Okewale and Adesina (2020). We polished 40 x 20 x 0.5 mm mild steel coupons with abrasive paper, lubricated them to prevent corrosion, degreased them with ethanol, rinsed them with distilled water, and dried them. In 100 mL beakers containing 50 mL of produced water and different inhibitor doses (a water-based inhibitor and moringa leaf extract), the manufactured mild steel coupons were suspended. At 30°C, the inhibitor concentrations that were employed were 0/100 ppm, 25/75ppm, 50/50ppm, 75/25 ppm, and 100/0ppm. The vouchers were submerged for 2, 4, 6, 8, and 10 days. After each corrosion study, the mild steel coupons were removed, rinsed with distilled water, and placed in a methanol solution to remove residual acids and inhibitors. The coupons were further washed with an appropriate cleaning solution, rinsed with distilled water, and dried in acetone before being reweighed.

The weight loss of the mild steel coupon was calculated using the equation below;

$$\text{Weight loss, (g)} = W - W_i \quad (1)$$

Where W is the initial weight of the mild steel coupon, and W_i is the weight of the mild steel coupon after the corrosion study. The corrosion rate was calculated using equation 2:

$$CR = \frac{87.6W}{At\rho} \quad (2)$$

Where; w =Corrosion weight loss of carbon steel (mg), A =The total surface area of the specimen in (cm^2), t = The exposure time in hours (h), ρ =The density of the specimen (g/cm^3)

2.4 Adsorption Isotherms

This study tested three adsorption isotherms to understand the interface between the inhibitor and the carbon steel surface. The coefficient of determination (R^2) from linear regression was used to determine the model that best fit the experimental values.

2.4.1 Langmuir isotherm

The equation represents the Langmuir relationship

$$\frac{C}{\theta} = \frac{1}{K_{ads}} + C \quad (3)$$

where: K_{ads} is the adsorption equilibrium constant (ppm^{-1}, equivalent to L mg-1), which was employed to obtain the Gibbs' free energy; C is the inhibitor concentration ppm; and Θ is the degree of surface coverage

2.4.2 Freundlich isotherm

This is expressed in the equation

$$\theta = KCn \quad (4)$$

Equation (8) can be rewritten as;

$$\ln\theta = \ln K + n\ln C \quad (5)$$

Where: Θ is the degree of surface coverage, C is the inhibitor concentration, in ppm, K is the adsorption constant, which is a measure of adsorption capacity (L/g), and n is the positive constant called the Freundlich exponent, which talks about the intensity of the adsorption process on the carbon steel surface (Okewale & Adebayo, 2020).

2.4.3 Temkin isotherm

This is expressed in the equation.

$$\theta = \frac{1}{f} \ln (KadsC) \quad (6)$$

This equation can be rewritten as;

$$\theta = \frac{1}{f} \ln C + \frac{1}{f}\ln K \quad (7)$$

where: Θ is a linear function of ln C, K is the equilibrium constant of adsorption (L/g), C is the inhibitor concentration (ppm), and f is a coefficient of inhomogeneity connected with the range of inhomogeneity C by equation (8) below

$$f = C/RT \quad (8)$$

2.5 Determination of the thermodynamic properties

The activation energy of the process was obtained using Equation (9), while the thermodynamic parameters, such as enthalpy and entropy of carbon steel corrosion inhibition in the produced water, were calculated using Equation (10), and the Gibbs' free energy was calculated using Equation (11). We used the transition state theory equation in Equation (5) (Okewale & Adebayo, 2020; Elijah et al., 2025).

$$\log CR = \log A - \frac{Ea}{2.303RT} \quad (9)$$

$$\text{Log}\left(\frac{CR}{T}\right) = \left[\log\left(\frac{R}{Nh}\right) + \frac{\Delta S^0}{2.303R}\right] - \frac{\Delta H}{2.303RT} \quad (10)$$

where: h is Planck's constant (6.626176 × 10^-34 J · s), N is Avogadro's number (6.022×10^{23} mol^{-1}), R is the Universal gas constant (8.314 J/K·mol), and T is the temperature of the medium. The Gibbs' free energy of adsorption ($\Delta G°_{ads}$), which can

characterize the interaction of adsorbed molecules and the metal surface

$$\Delta G°ads = -RT \ln (55.5 \times k_{ads}) \quad (11)$$

where: k_{ads} is the adsorption equilibrium constant, R is the gas constant (8.314 J/mol · K), T is the absolute temperature in Kelvin, and 55.5 is the concentration of water in solution expressed in mol/L.

3.0 Results and Discussion

3.1 Surface Morphology Analysis

Scanning electron microscope (SEM) images were taken to study the surface morphology of carbon steel in the absence and presence of moringa leaf extract inhibitor. Figure 1 below shows the SEM-EDX analysis of the mild steel sample, conducted in the absence of an inhibitor or corrosive medium

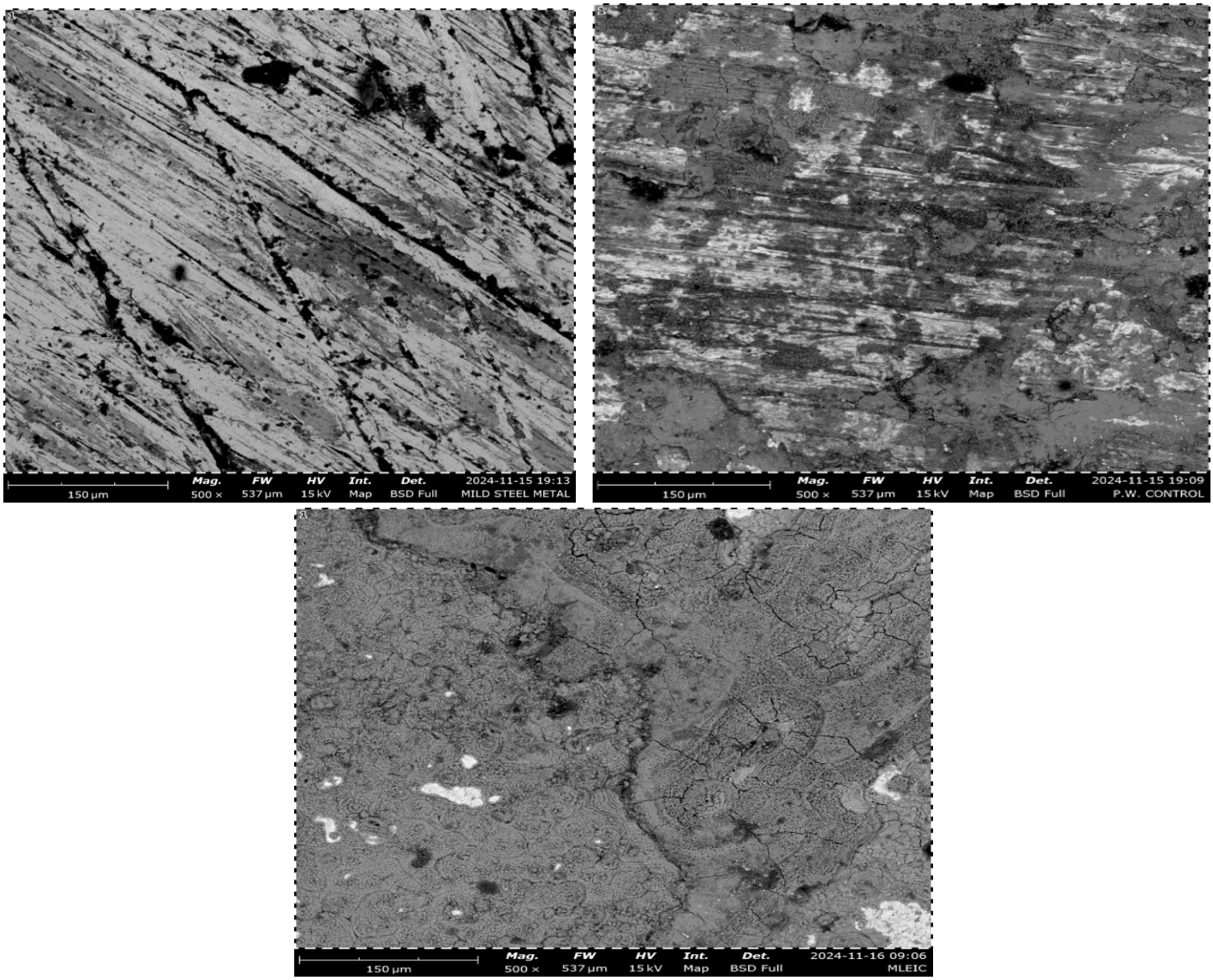

Figure 1: (a) SEM-EDX of mild steel coupon, (b) SEM-EDX of mild steel in produced water (control), and (c) SEM analysis of the MLE inhibitor

Table 1: EDX composition of mild steel coupon

Element Number	Element Symbol	Element Name	Atomic Conc.	Weight Conc.
26	Fe	Iron	91.47	97.03
6	C	Carbon	6.42	1.46
20	Ca	Calcium	0.67	0.51
19	K	Potassium	0.45	0.33
17	Cl	Chlorine	0.48	0.32
16	S	Sulphur	0.35	0.21
25	Mn	Manganese	0.07	0.07
15	P	Phosphorus	0.08	0.05
13	Al	Aluminium	0.00	0.00
14	Si	Silicon	0.00	0.00
12	Mg	Magnesium	0.00	0.00
11	Na	Sodium	0.00	0.00
22	Ti	Titanium	0.00	0.00

Table 2: EDX composition of mild steel in produced water (control)

Element Number	Element Symbol	Element Name	Atomic Conc.	Weight Conc.
26	Fe	Iron	91.47	97.03
6	C	Carbon	6.42	1.46
20	Ca	Calcium	0.67	0.51
19	K	Potassium	0.45	0.33
17	Cl	Chlorine	0.48	0.32
16	S	Sulphur	0.35	0.21
25	Mn	Manganese	0.07	0.07
15	P	Phosphorus	0.08	0.05
13	Al	Aluminium	0.00	0.00
14	Si	Silicon	0.00	0.00
12	Mg	Magnesium	0.00	0.00

11	Na	Sodium	0.00	0.00
22	Ti	Titanium	0.00	0.00

In Figure 1, the SEM-EDX analysis of the mild steel sample, conducted without an inhibitor or corrosive medium, provides crucial insights into its surface morphology and elemental composition. The SEM image reveals a relatively smooth surface, characteristic of unaltered mild steel. The absence of significant pitting confirms that the sample was not exposed to corrosive environments, affirming its integrity before experimentation. The SEM-EDX analysis of mild steel exposed to produced water without the Moringa leaf extract inhibitor demonstrates significant surface degradation and elemental changes due to corrosion. The SEM image reveals pronounced surface irregularities, including pits and grooves, characteristic of severe corrosion activity. These features suggest that the chloride-rich produced water environment promotes localized and uniform corrosion by disrupting the steel's passive oxide layer. SEM analysis of mild steel exposed to produced water with the Moringa leaf extract (MLE) inhibitor shows the inhibitor's protective effect in mitigating corrosion, with a noticeably smoother surface than the untreated control sample. While minor grooves were present, the absence of significant pits or cracks indicates that the MLE effectively forms a barrier against corrosive agents, reducing damage to the steel surface.

The EDX analysis highlights a dominant iron (Fe) concentration of 88.37% by weight, confirming that the steel remains largely intact. The presence of sulfur (S) and chlorine (Cl) at lower concentrations (2.52% and 0.94%, respectively) than in the control sample indicates the inhibitor's role in minimizing their corrosive impact. The detection of carbon (C) at 0.73% indicates organic residues from the MLE, which contribute to forming a protective layer. Other elements, such as sodium (Na), aluminum (Al), and silicon (Si), are present in trace amounts, likely residual from the produced water or the inhibitor itself.

The EDX data, summarized in Table 1, confirm that the sample is predominantly iron (Fe), with a weight concentration of 97.03%. Carbon (C) is the second most prominent element, reflecting its role in the steel's structure and mechanical properties. Trace elements such as calcium (Ca), potassium (K), chlorine (Cl), and sulfur (S) were detected, albeit in minimal quantities. These traces could stem from manufacturing processes or environmental exposure during storage. Notably, elements such as silicon (Si), magnesium (Mg), and titanium (Ti) were either absent or present below detectable limits, underscoring the purity of the mild steel sample. However, the EDX data quantitatively confirm the impact of corrosion, with iron (Fe) concentration reduced to 89.19% compared to untreated steel. Chlorine (Cl) is present at 0.99%, indicating its role in pitting and accelerating corrosion. Sulfur (S) at 0.84% suggests iron sulfide formation, common in environments containing sulfates or hydrogen sulfide (H_2S). Other detected elements, such as silicon (Si) and aluminum (Al), may be impurities or residues introduced during corrosion. Trace elements such as calcium (Ca) and potassium (K) further indicate interactions with ionic species in the corrosive medium.

3.2 FTIR spectrum of the water-based inhibitor (WBI) and MLE

FTIR was used to determine the chemical composition of the Moringa leaf extract and the water-based inhibitor, elucidating their corrosion inhibition properties through interactions with the mild steel surface. The FTIR spectrum of the Moringa leaf extract (MLE) in Figure 2 below provides critical insights into its chemical composition and potential as a green corrosion inhibitor.

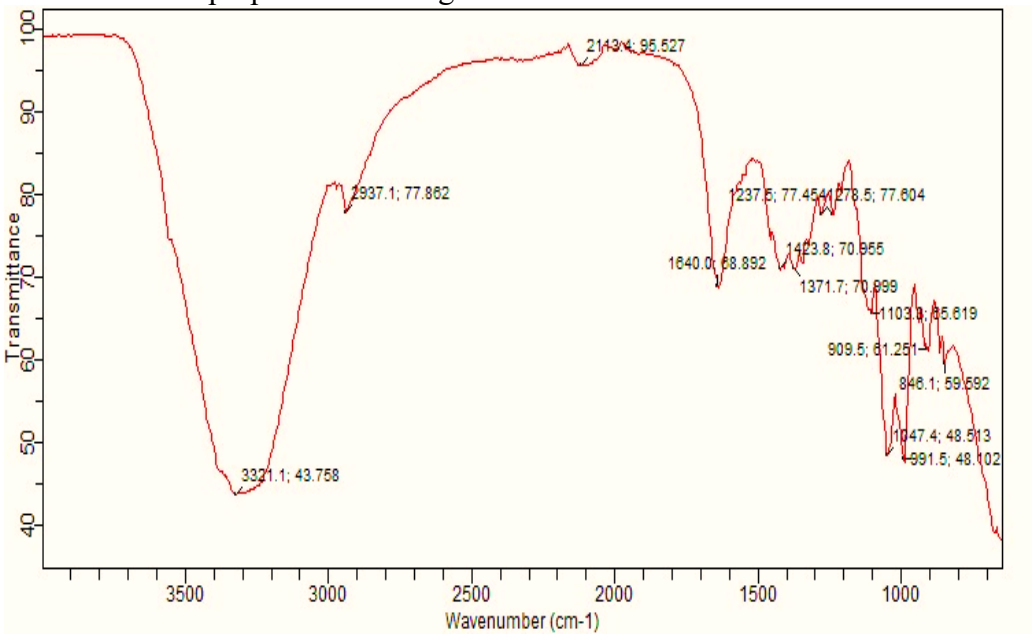

Figure 2(a): The FTIR results for the water-based inhibitor

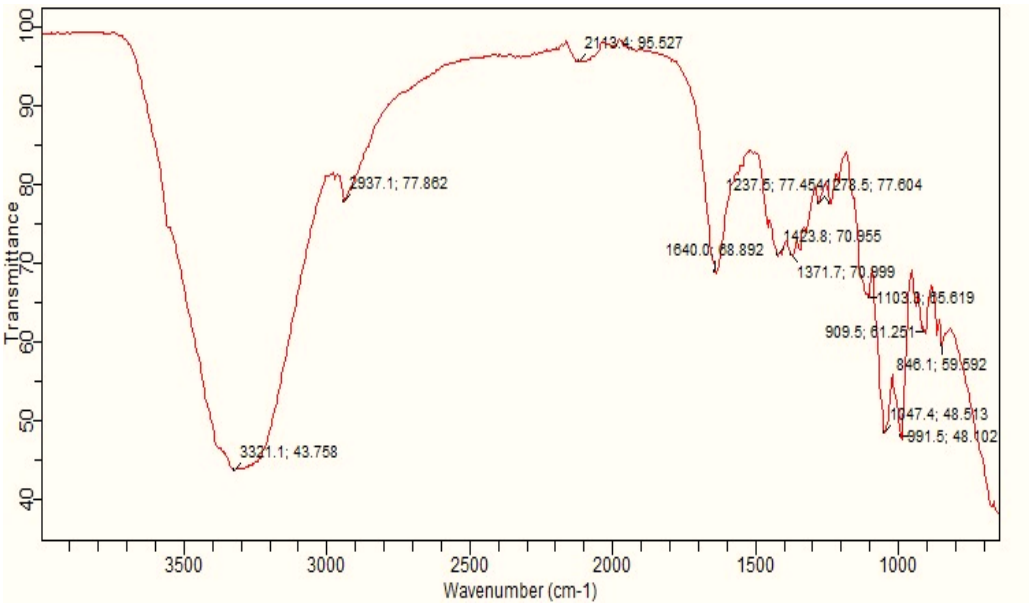

Figure 2(b): The FTIR results for moringa leaf extract (MLE)

A strong, broad peak at 3261 cm^{-1} is attributed to O–H stretching vibrations, indicating hydroxyl groups in phenolic and alcoholic compounds. These groups play a vital role in corrosion inhibition by forming hydrogen bonds with the mild steel surface, promoting a stable protective film. This aligns with previous studies that identify phenolic compounds as effective inhibitors because they interact with metal surfaces through adsorption (Wei et al., 2021).

The peak at 2928 cm^{-1} corresponds to C–H stretching vibrations in aliphatic compounds. These hydrophobic groups enhance the extract's ability to repel water, reducing mild steel's exposure to corrosive agents such as oxygen and chloride ions. The weak signal at 2109 cm^{-1}, indicative of C≡N or C≡C groups, suggests the presence of nitriles or alkynes, which exhibit high chemical affinity for the metal surface, thereby strengthening the adsorption process (Wu et al., 2022).

Additionally, the distinct peak at 1638 cm^{-1} is associated with carbonyl (C=O) groups, typically found in esters, ketones, or amides. These functional groups interact with the steel surface through lone pair electrons, enhancing the protective film's adhesion. Peaks in the 1513–1238 cm^{-1} region indicate aromatic and etheric compounds, which provide corrosion resistance through π-electron interactions with the metal surface (Singh et al., 2023). Finally, peaks at lower wavenumbers (920–1017 cm^{-1}) correspond to C–O stretching vibrations, which may be linked to esters or polysaccharides. These functional groups further contribute to the extract's ability to form a dense barrier that shields the metal surface from corrosive media.

In summary, FTIR analysis of MLE confirms the presence of functional groups, including hydroxyl, carbonyl, aromatic, and aliphatic compounds, which collectively contribute to its corrosion-inhibiting properties. These findings complement the phytochemical analysis results, which reveal a rich composition of bioactive compounds, including phenols, flavonoids, and alkaloids. Such a diverse chemical profile makes MLE a promising eco-friendly alternative for combating corrosion in mild steel applications (Ahamad et al., 2020; Wei et al., 2021; Wu et al., 2022).

3.3 Blended Inhibitor Performance

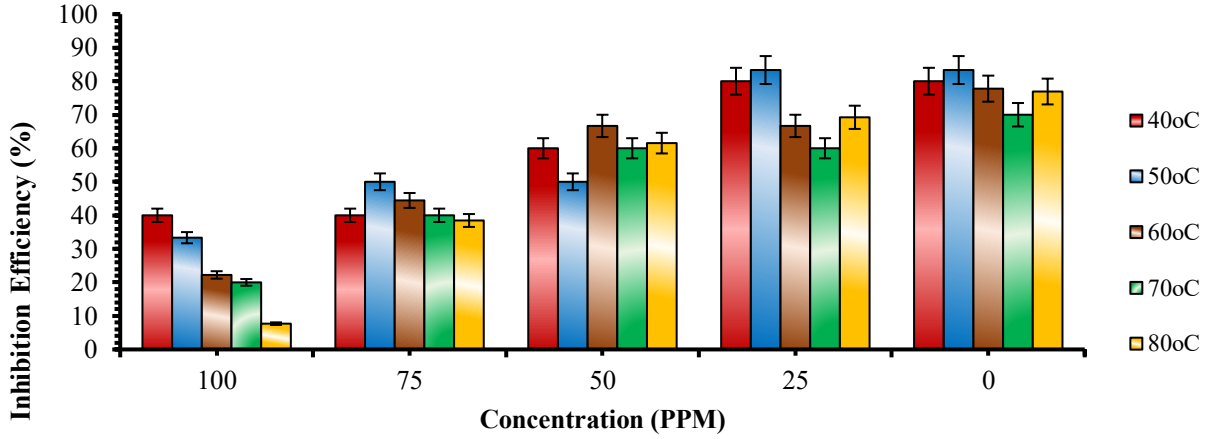

Figure 3. Effect of Inhibitor Concentration on the (a) Efficiency, (b) Surface coverage, and (c)

The blended inhibitors (e.g., 50/50 and 25/75 ppm)

As shown in Figure 3, the illustration shows optimal performance across a range of temperatures. At 60°C, the 50/50 blend achieves 66.67% inhibition efficiency. At 70°C, the 25/75 blend maintains the same efficiency and outperforms both pure synthetic and pure MLE inhibitors. This suggests that blending enhances thermal stability and improves performance under varying temperature conditions, as observed in similar studies on inhibitor synergy (Singh et al., 2023; Shukla et al., 2019).

The inhibition efficiency (% IE) generally decreases with increasing temperature across all inhibitor blends. At lower temperatures, such as 40°C and 50°C, blends with higher Moringa leaf extract (MLE) content (e.g., 0/100 ppm) achieve higher inhibition efficiencies (up to 83.33% at 50°C). This efficiency corresponds to higher surface coverage (θ), indicating that a greater proportion of the mild steel surface is protected at these temperatures.

At elevated temperatures (70°C and 80°C), inhibition efficiency declines significantly, with pure MLE achieving only 70% at 70°C and 76.92% at 80 °C. This trend suggests that the inhibitor molecules desorb from the steel surface as the temperature increases, weakening the protective barrier. The adsorption of bioactive compounds from MLE onto the metal surface is typically physisorptive and less stable at higher temperatures, consistent with earlier studies (Wei et al., 2021; Wu et al., 2022). The corrosion rate increases with temperature across all inhibitor concentrations, reflecting the thermally activated nature of the corrosion process. For instance, at 40°C, the control sample (no inhibitor) has a corrosion rate of 0.331 mm/year, which increases to 0.861 mm/year at 80 °C. However, the inhibitors significantly reduce the corrosion rate. For example, at 80 °C, the 0/100 ppm blend achieves a corrosion rate of 0.199 mm/year, which is considerably lower than that of the control. This reduction is attributed to inhibitor-formed protective films, although their effectiveness diminishes at higher temperatures. The combination of MLE with synthetic inhibitors exhibits a synergistic effect, particularly at lower temperatures, thereby enhancing both thermal stability and adsorption capacity.

3.4 Adsorption Isotherms

Table 3: Adsorption corrosion inhibition isotherm constants and coefficients of determination at the various temperatures.

Temperature (K)	Langmuir K_{ads} (L/g)	R^2	Freundlich K_{ads} (L/g)	R^2	Temkins K_{ads} (L/g)	R^2
313	0.059999	0.9113	0.073181	0.9611	0.145297	0.9584
323	0.0625	0.8634	0.118631	0.7403	0.203285	0.7403
333	0.084846	0.9581	0.13555	0.9143	0.315098	0.9235
343	0.076365	0.9581	0.121983	0.9143	0.315051	0.9235
353	0.061538	0.9311	0.080334	0.9638	0.169854	0.9873

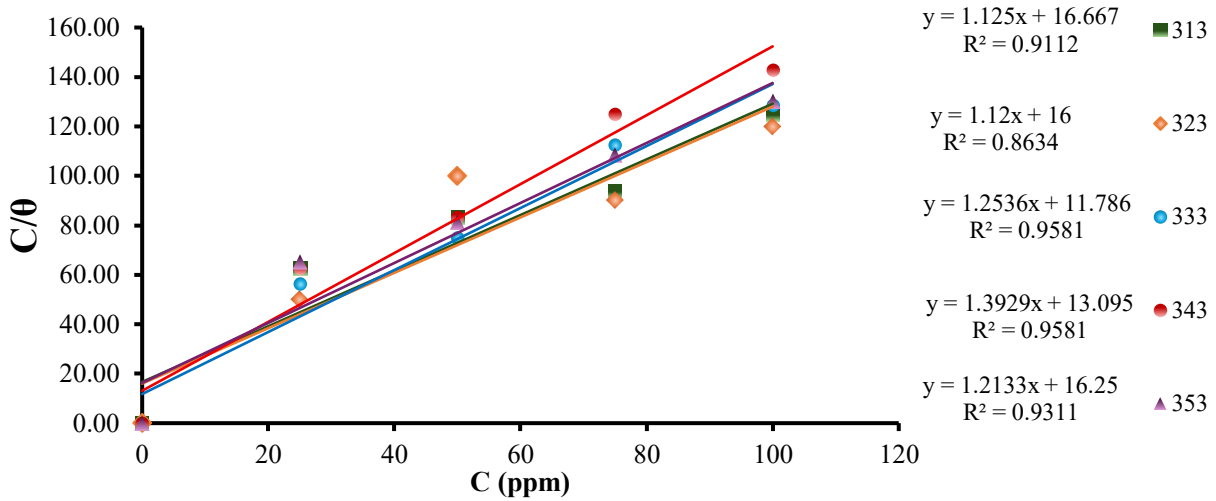

Figure 4(a): Corrosion Inhibition isotherm traces showing Langmuir model fit,

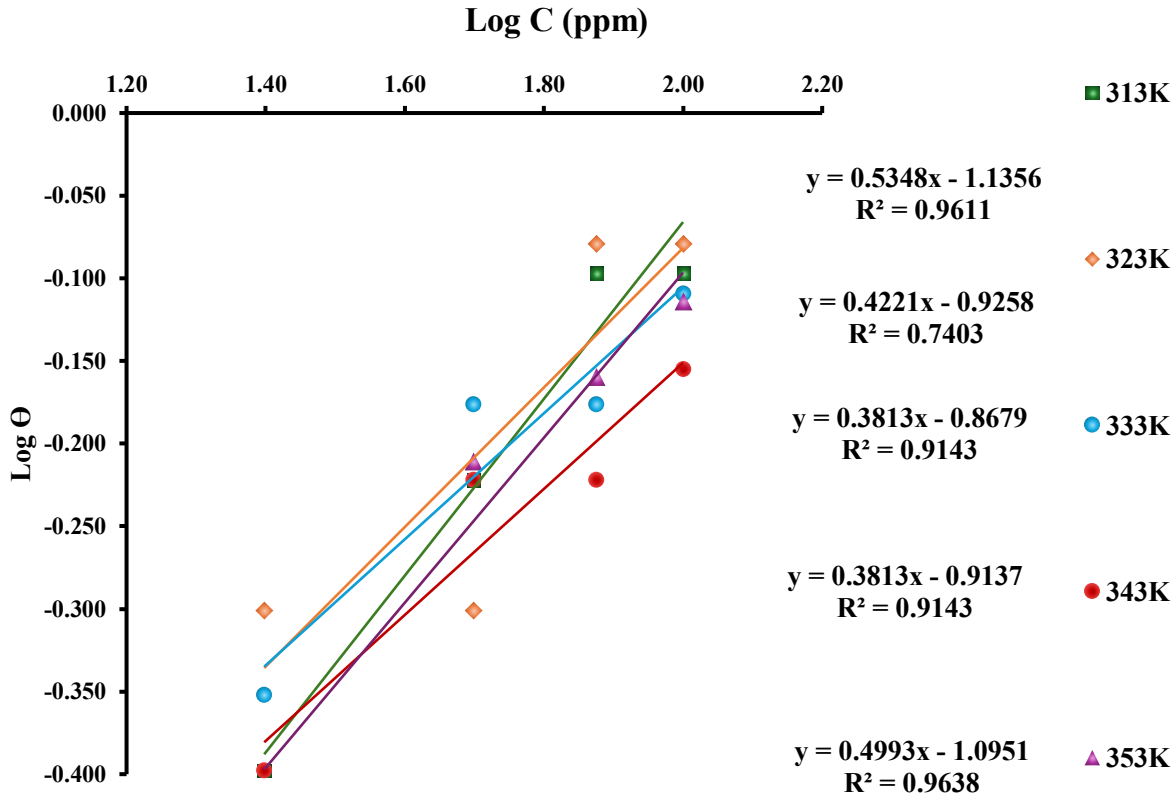

Figure 4(b): Corrosion Inhibition isotherm traces showing Freundlich isotherm model fit,

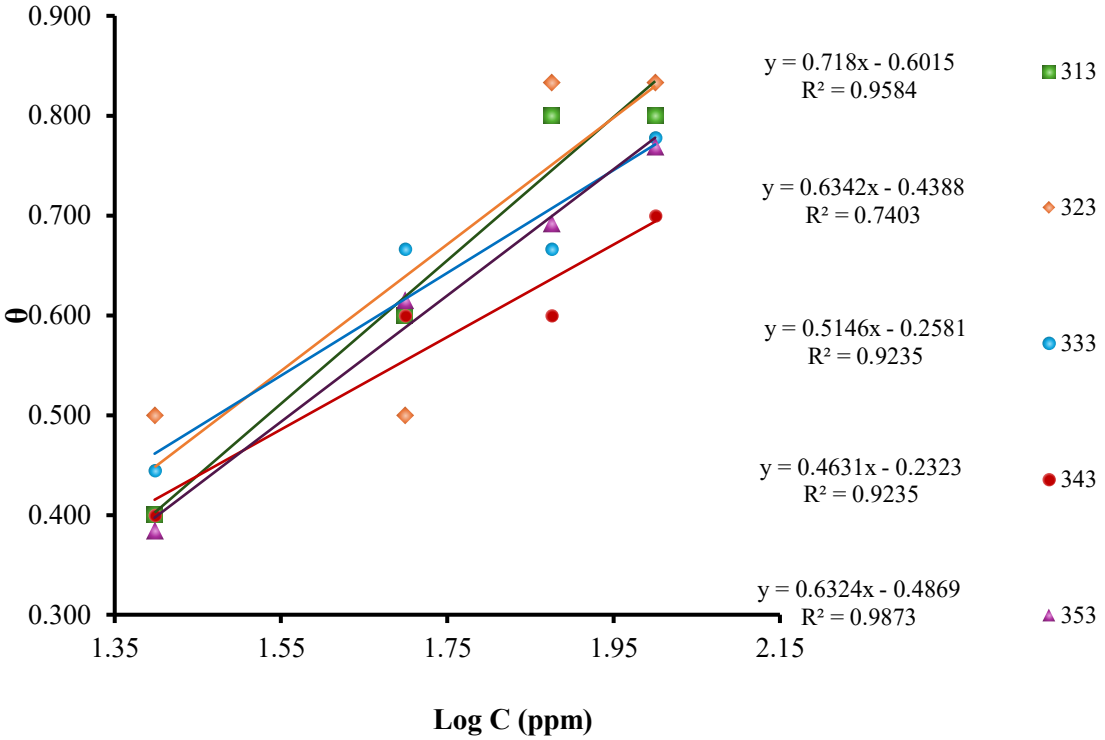

Figure 4(c): Corrosion Inhibition isotherm traces showing Temkin's model fit

Together, the graph and table provide evidence that the adsorption process follows the Langmuir isotherm model. Table 3 presents the various parameters of the adsorption isotherms studied. The adsorption equilibrium constant (Kads) decreased with increasing temperature, indicating that the inhibitor adsorbs more readily onto the carbon steel surface at lower temperatures. Conversely, at higher temperatures, the adsorbed inhibitor tends to desorb from the carbon steel surface. These findings are consistent with the results reported by Manimegalai and Manjula (2015). The Langmuir adsorption isotherm suggests that the PPE extract contains organic compounds with polar atoms or groups that are adsorbed onto the metal surface, potentially interacting through mutual repulsion or attraction.

The 50/50 blend showed balanced performance with moderate Ea and effective inhibition across temperatures, while the 25/75 blend showed superior thermal stability, making it more suitable for high-temperature conditions. The performance of MLE-only (0/100) is comparable to that of synthetic-only (100/0), demonstrating the effectiveness of bio-based inhibitors.

The data and graph collectively emphasize the synergistic benefits of blending Moringa leaf extract (MLE) with synthetic inhibitors. The blends effectively lower Ea and maintain protective efficiency at higher temperatures by forming stable adsorbed layers on the metal surface. This behaviour makes blended inhibitors suitable for challenging industrial conditions, such as in oilfield systems (Wei et al., 2021; Wu et al., 2022).

3.5 Thermodynamics Studies

The graph plots log (C_R) (corrosion rate) against 1/T (inverse temperature), illustrating the temperature dependence of the corrosion process.

Table 4. Activation energy, enthalpy, and entropy at various concentrations of the inhibitor.

Inhibitor Conc (ppm)	E_a (kJ/mol)	ΔH^o (KJ/mol)	ΔS^o (J/mol K)	Langmuir ΔG ($KJmol^{-1}$)	Freundlich ΔG ($KJmol^{-1}$)	$E_a - \Delta H^o$
100/0	31.872	29.109	-165.921	-3.13042	-3.64727	2.763
75/25	24.302	21.541	-190.887	-3.34011	-5.06108	2.761
50/50	19.492	16.729	-186.857	-4.28981	-5.58687	2.763
25/75	38.392	35.631	-154.826	-4.11829	-5.45391	2.761
0/100	30.327	27.566	-180.720	-3.60484	-4.38707	2.761
Control	22.274	19.511	-192.352	-	-	2.763

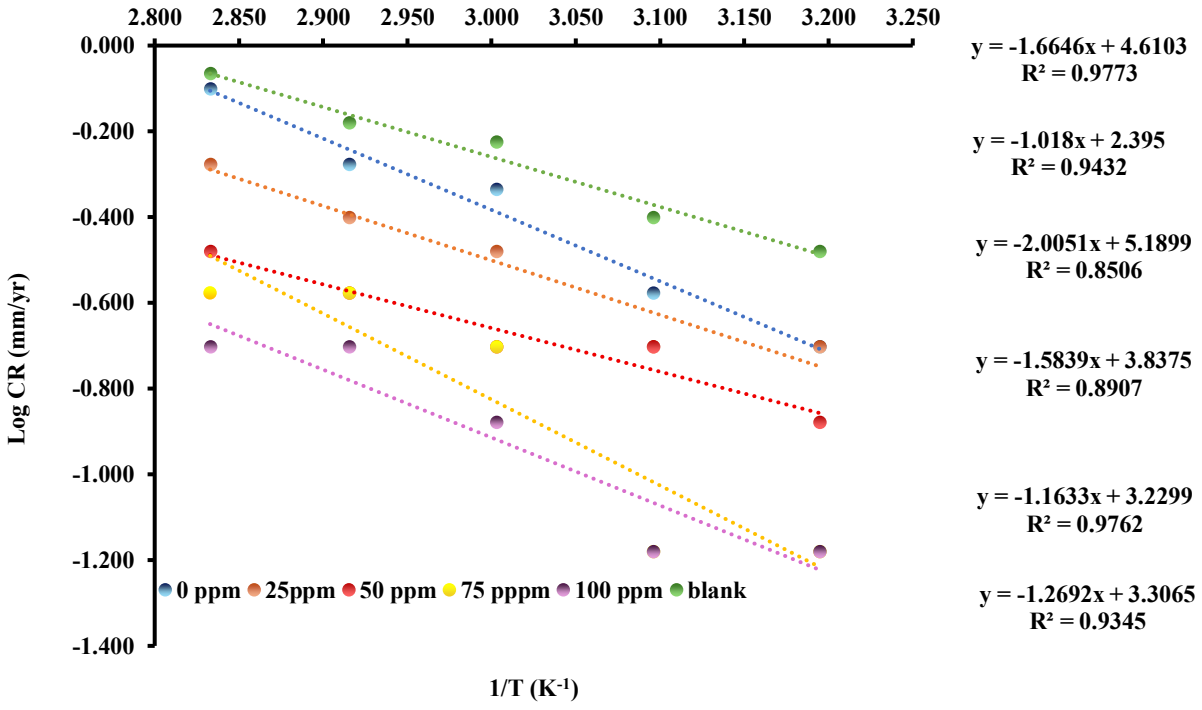

Figure 5(a): Graph of LogCR(mm/yr) against 1/T

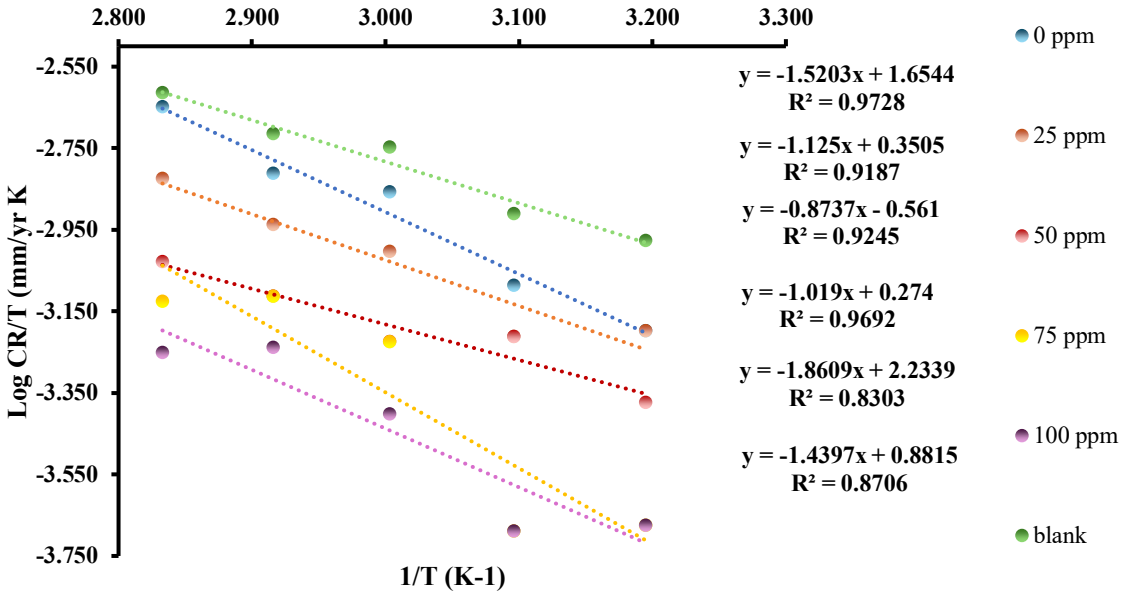

Figure 5(b): Graph of Log C_R/T(mm/yr K) against 1/T.

The linear regression trends indicate adherence to the Arrhenius equation, confirming the reaction's temperature-driven nature. Higher slopes correlate with higher activation energy values, as seen in the 25/75 blend (steeper slope), which provides better temperature resistance. The blank (control) shows the steepest increase in corrosion rate with temperature, reinforcing the protective role of inhibitors.

The activation energy (Ea) values represent the energy barrier the corrosion reaction must overcome to proceed. The table shows that activation energy varies with inhibitor concentration. For instance, the Ea for the 50/50 blend is the lowest (19.492 kJ/mol), indicating that this blend effectively lowers the corrosion reaction rate by forming a strong adsorptive protective film. The Ea for the 25/75 blend is the highest (38.392 kJ/mol), suggesting enhanced thermal stability and stronger inhibitor adsorption at this concentration. The control sample (no inhibitor) shows a moderate Ea (22.274 kJ/mol), indicating that, without an inhibitor, the corrosion process proceeds relatively unhindered. These findings align with the literature, which emphasizes the influence of inhibitor concentration on the activation energy of mild steel in corrosive environments (Ahamad et al., 2020). The slight discrepancies (Ea − ΔH^o approx 2.76) across all samples indicate consistent energy-barrier transition states for the corrosion process, confirming that the inhibitors primarily alter adsorption efficiency rather than the reaction mechanism.

The enthalpy change represents the heat absorbed or released during the corrosion process. All ΔH^o values are positive, confirming that the corrosion process is endothermic and requires energy to proceed. The 25/75 blend has the highest ΔH^o (35.631 kJ/mol), indicating a stronger barrier to corrosion. The 50/50 blend shows a slightly lower ΔH^o (16.729 kJ/mol), suggesting that although the reaction still requires energy, inhibitor adsorption compensates for some of the energy demand.

The entropy (ΔS^o) values are negative across all concentrations, indicating decreased

disorder at the interface due to inhibitor adsorption onto the steel surface. The 25/75 blend exhibits the least negative ΔSº value (-154.826 J/mol·K), indicating adsorption and adequate surface coverage. Conversely, the control sample has the most negative ΔSº (-192.352 J/mol·K), consistent with uninhibited corrosion, where metal ions freely dissolve into the solution. Adsorption capacity decreases with increasing temperature, indicating an exothermic process. The negative ΔG values confirm the spontaneity of the adsorption process.

4.0 Conclusion

The study showed that combining Moringa leaf extract (MLE) with a water-based corrosion inhibitor (WBI) effectively reduces corrosion in mild steel when exposed to produced water. Inhibition efficiency can reach up to 83.33% at lower temperatures (40–50°C) with higher MLE blends; however, it drops significantly at elevated temperatures (70–80 °C) due to inhibitor desorption and reduced surface coverage. As temperatures rise, the corrosion rate tends to increase. Still, the blended formulations show better inhibition, leading to improved thermal stability and lower corrosion rates (for instance, 0.199 mm/yr at 80 °C for a 0/100 ppm blend) than the controls. FTIR analysis confirms the presence of functional groups (such as O–H and C=O) that facilitate adsorption and film formation. In summary, these eco-friendly blends offer a promising, sustainable option for corrosion protection in oil and gas settings, particularly under moderate conditions, with optimal performance at balanced ratios. The kinetic and thermodynamic study of *Moringa Oleifera* Leaf Extract (MLE) and a water-based corrosion inhibitor demonstrates their effectiveness in mitigating mild steel corrosion in produced water. The 25/75 blend of MLE and synthetic inhibitor exhibited the highest activation energy (38.392 kJ/mol), indicating superior thermal stability and strong adsorption, making it suitable for high-temperature industrial environments. The 50/50 blend, with the lowest activation energy (19.492 kJ/mol), provided balanced inhibition efficiency across various temperatures. Thermodynamic analysis confirmed an endothermic corrosion process with negative entropy changes, reflecting ordered inhibitor adsorption on the steel surface. The Langmuir adsorption isotherm best describes the adsorption behavior, with negative Gibbs free energy values indicating spontaneous, exothermic adsorption. SEM-EDX analysis revealed smoother surfaces and reduced concentrations of corrosive elements in the presence of MLE, underscoring its role in forming protective films. The synergistic effects of MLE and synthetic inhibitors highlight their potential as eco-friendly, cost-effective solutions for corrosion control in oil and gas applications. Further studies should explore the long-term performance and scalability of these inhibitors in real-world conditions.

References

Afoegba, C.S., Agbonkhese, K., & Onobrenufe, O. (2020). Influence of PH, Immersion Time and Inhibitor Concentration on the Corrosion Inhibition Characteristic of Citrullus Lanatus Extract on A36 Carbon Steel in A CO2 Saline Solution. *International Journal of Advances in Scientific Research and Engineering (ijasre),* 6(12), pp. 56–74.

Aghogho, E. E., Ovuoraye, P. E., Oboh, I. O., & Olayebi, O. O. (2025). Exploring the potential of mango-orange leaf extract as an inhibitor on carbon steel in an acidic medium: Optimization, kinetics, and thermodynamics. *Next Materials,* 8, 100898.

https://doi.org/10.1016/j.nxmate.2025.100898

Ahamad, I., Prasad, R., & Quraishi, M. A. (2020). Inhibitive effect of naturally occurring plant extracts on the corrosion of mild steel in acidic media. *Corrosion Science,* 54(1), 1–5. https://doi.org/10.1016/j.corsci.2020.101564

Akalezi, C.O., Maduabuchi, A.C., Enenebeaku, C.K., & Oguzie (2020). Experimental and DFT evaluation of adsorption and inhibitive properties of *Moringa oleifera* extract on mild steel corrosion in acidic media. *Arabian Journal of Chemistry*, 13, 9270–9282.

Azeem, M., Pirjan, K., Qasim, M., Mahmood, A., Javed, T., Muhammad, H., Yang, S., Dong, R., Ali, B., & Rahimi, M. (2023). Salinity stress improves antioxidant potential by modulating physio-biochemical responses in moringa oeifera Lam. Scientific Reports, 13, 2895

Dehghani, A., Ghahremani, P., Mostafatabar, A. H., & Ramezanzadeh, B. (2024). Plant extracts: Probable alternatives for traditional inhibitors for controlling alloy corrosion against acidic media—A review. *Biomass Conversion and Biorefinery*, *14*(6), 7467–7486.

Didouh, H., Buyuksagis, A., Hadj Meliani, M., Dilek, M., Kayali, Y., Suleiman, R. K., & Saleh, T. A. (2023). Investigating the use of Moringa Oleifera leaf extract as an environmentally friendly corrosion inhibitor for API 5L X52 steel in 1 M HCl. *Journal of Molecular Liquids*, *390*, 122910.

Emmanuel, J.K. (2024). Corrosion protection of mild steel in corrosive media, a shift from synthetic to natural corrosion inhibitors: A review. Bulletin of the National Research Centre, 48, 26

Fedorowicz, J., & Saczewski, J. (2024). Advances in the synthesis of biologically active quaternary ammonium compounds. *International journal of molecular sciences.* 25(9), 4649.

Fouda, A. S., Ahmed, A. M., El-Darier, S. M., & Ibrahim, I. M. (2021). Moringa oleifera as an Eco-friendly corrosion inhibitor for carbon steel in hydrochloric acid solution. *International Journal of Corrosion and Scale Inhibition*, 10(4), 1456–1475.

Ituen, E., Akaranta, O., & James, A. (2017). Evaluation of Corrosion Inhibitor Performance Using Adsorption Isotherm Models: An Overview. *Chem. Sci. Int. J*, *18*(1), 1-34.

Jain, P., Sharma, M., Dureja, P., Sarma, P. M., & Lal, B. (2017). Bioelectrochemical approaches for the removal of sulfate, hydrocarbon, and salinity from produced water. *Chemosphere*, *166*, 96–108.

Manimegalai, S., & Manjula, P. (2015). Thermodynamic and adsorption studies for corrosion inhibition of mild steel in aqueous media by *Sargasam swartzii* (brown algae). *J. Mater. Environ. Sci*, *6*(6), 1629–1637.

Mustapha, S., Elabor, R., Amigun, A. T., Etsuyankpa, M. B., Egbosiuba, T. C., Shuaib, D. T., & Mohammed, A. K. (2024). Phytochemicals/Plant Extracts as Corrosion Inhibitors for Zinc in Various Electrolytes. In *Phytochemistry in Corrosion Science* (pp. 263–295). CRC Press.

Njoku, C. N., Maduoma, T. U., Emori, W., Odey, R. E., Unimke, B. M., Yakubu, E., ... and Oyoh, K. B. (2024). Natural and Synthetic Drugs as Eco-Friendly and Sustainable Corrosion Inhibitors for Metals: A Review. *Pigment & Resin Technology*, *53*(6), 1074–1087.

Nwigbo, S. C., Okafor, V. N., & Okewale, A. O. (2012). Comparative study of Elaeis guineensis Exudates (palm wine) as a corrosion inhibitor for mild steel in acidic and basic solutions. *American Journal of Materials Science*, 2(4), 122–126

Nyangiwe, N. N. (2025). Exploring Corrosion Inhibitor Adsorption on Metal Surfaces through Density Functional Theory and Molecular Dynamics Simulations. In *The Challenges of Corrosion Control on Metallic Surfaces*. Intech Open. https://doi.org/10.5772/intechopen.1009688

Okewale, A. O., & Adesina, O. A. (2020). Kinetics and thermodynamic study of corrosion inhibition of mild steel in a 1.5 M HCl medium using cocoa leaf extract as an inhibitor. *Journal of Applied Sciences and Environmental Management*, 24(1), 37. https://doi.org/10.4314/jasem.v24i1.6

Popoola, L. T., Grema, A. S., Latinwo, G. K., Gutti, B., & Balogun, A. S. (2013). Corrosion Problems during Oil and Gas Production and Their Mitigation. *International Journal of Industrial Chemistry*, *4*(1), 35.

Prasad, A.P., Kunyankandy. A., and Joseph, A. (2020). Corrosion inhibition of the oil and gas industry. *Willey* http://doi.org/10.1002/9783527822140.ch5

Quadri, T. W., Akpan, E. D., Olasunkanmi, L. O., Fayemi, O. E., & Ebenso, E. E. (2022). Fundamentals of corrosion chemistry. In *Environmentally sustainable corrosion inhibitors* (pp. 25–45). Elsevier.

Shukla, S. K., Singh, A. K., Pandey, A. K., & Sinha, P. (2019). Corrosion inhibition and adsorption Behaviour of *Clerodendrum colebrookianum Walp* leaves extract on cold-rolled steel in 1 M H2SO4 solution. *Journal of Bio- and Tribo-Corrosion*, 5(3), 1–14.

Singh, A. K., Chugh, B., Thakur, S., Pani, B., Lgaz, H., Chung, I. M., and Chaubey, R. (2023). Green approaches in the synthesis of 12-tungstophosphoric acid-impregnated iron and cerium-doped mesoporous silica catalysts: Recycling of agricultural waste for biodiesel production from waste cooking oil. *ACS Sustainable Chemistry & Engineering*, 11(3), 1199–1213.

Toghan, A., Gadow, H. S., Fawzy, A., Alhussain, H., & Salah, H. (2023). Adsorption mechanism, kinetics, thermodynamics, and anticorrosion performance of a new thiophene derivative for C-steel in a 1.0 M HCl: experimental and computational approaches. *Metals*, *13*(9), 1565.

Udounwa, A. E., & Wilson, E. O. (2025). Corrosion of Thermo-Mechanically Treated (TMT) Mild Steel in Reinforced Concrete Structures: Mechanical and Structural Implications. *Journal of Applied Ecology and Environmental Design*. *9*(4). https://doi.org/10.70382/hujaeed.v9i4.009

Wei, W., Zhang, J., & Xie, Q. (2021). Corrosion and protection of mild steel in produced water: The effect of environmental parameters. *Corrosion Science,* 182, 109247. https://doi.org/10.1016/j.corsci.2020.109247

Wu, Z., Zhang, Y., & Xie, Y. (2022). The impact of natural inhibitors on the corrosion of mild steel in produced water: A comparative study of plant extracts. *Corrosion Reviews,* 40(3), 217–233. https://doi.org/10.xxxx/corr.rev.2022.0117

Zhang, M., Chen, Y., Liu, & Zhuo, K. (2023). Artemisia capillaris leaf extract as a corrosion inhibitor for Q235 Steel in HCL solution and its synergistic inhibition effect with L-cysteine. *ChemElectroChem*, 10(10).